

Design of an Oligosaccharide Scaffold That Binds in the Minor Groove of DNA

Hayley Xuereb, Milana Maletic, Jeff Gildersleeve, István Pelczer, and Daniel Kahne*

Contribution from the Department of Chemistry, Princeton University, Princeton, New Jersey, 08544

Received July 16, 1999

Abstract: Many biological recognition events involve extensive interactions between macromolecules. Strategies to design compounds that mimic large peptides or other elements of secondary structure could be useful for blocking interactions between large surfaces. In this paper, the use of oligosaccharides as scaffolds for the design of peptidomimetics is addressed. A functionalized oligosaccharide modeled after a basic region peptide helix has been designed and synthesized. This oligosaccharide binds to duplex DNA with micromolar affinity. The mode of binding has been established by 2D NMR, and shows that the oligosaccharide binds DNA in the minor groove with one surface of the oligosaccharide contacting the floor of the DNA.

Introduction

Biomolecular recognition events such as protein–protein and protein–DNA interactions typically involve contacts over a large surface area. For example, it is quite common for an α helix in a protein to contact another molecule over its entire length. There are no clear prescriptions for how to design compounds that block interactions between large surfaces, and this is one of the most challenging problems facing researchers interested in problems of molecular recognition. The obvious strategy is to design compounds that mimic peptide α helices or other elements of secondary structure. Some of the most exciting work in the area involves the use of polymers composed of β amino acids that fold into stable secondary structures.^{1,2} Gellman and others have been exploring strategies to stabilize helical β peptides in water, and it seems likely that these structures can be functionalized to serve as mimetics of more standard polypeptides.^{2m,n,p}

(1) For a review of engineered biopolymers with well-defined folding properties, see: Gellman, S. *Acc. Chem. Res.* **1998**, *31*, 173–180.

(2) For recent work in the area of biopolymer design, see: (a) Nicolaou, K. C.; Florke, H.; Egan, M. G.; Barth, T.; Estevez, V. A. *Tetrahedron Lett.* **1995**, *36*, 1775–1778. (b) Suhara, Y.; Ichikawa, M.; Hildreth, J. E. K.; Ichikawa, Y. *Tetrahedron Lett.* **1996**, *37*, 2549–2552. (c) Suhara, Y.; Izumi, M.; Ichikawa, M.; Penno, M. B.; Ichikawa, Y. *Tetrahedron Lett.* **1997**, *38*, 7167–7170. (d) Abele, S.; Guichard, G.; Seebach, D. *Helv. Chim. Acta* **1998**, *81*, 2141–2156. (e) Armand, P.; Kirshenbaum, K.; Goldsmith, R. A.; Farr-Jones, S.; Barron, A. E.; Truong, K. T.; Dill, K. A.; Mierke, D. F.; Cohen, F. E.; Zuckermann, R. N.; Bradley, E. K. *Proc. Natl. Acad. Sci. U.S.A.* **1998**, *95*, 4309–4314. (f) Hintermann, T.; Gademann, K.; Jaun, B.; Seebach, D. *Helv. Chim. Acta* **1998**, *81*, 983–1002. (g) Hanessian, T.; Luo, X.; Schaum, R.; Michnick, S. *J. Am. Chem. Soc.* **1998**, *120*, 8569–8570. (h) Kishenbaum, K.; Barron, A. E.; Goldsmith, R. A.; Armand, P.; Bradley, E. K.; Truong, K. T.; Dill, K. A.; Cohen, F. E.; Zuckermann, R. N. *Proc. Natl. Acad. Sci. U.S.A.* **1998**, *4303*–4308. (i) Smith, M. D.; Claridge, T. D. W.; Trnater, G. E.; Sansom, M. S.; Fleet, G. W. *J. Chem. Soc., Chem. Commun.* **1998**, 2041–2042. (j) Szabo, L.; Smith, B. L.; McReynolds, K. D.; Parill, A. L.; Morris, E. R.; Gervay, J. *J. Org. Chem.* **1998**, *63*, 1074–1078. (k) Yang, D.; Qu, J.; Li, B.; Ng, F.; Wang, X.; Cheung, K.; Wang, D.; Wu, Y. *J. Am. Chem. Soc.* **1999**, *121*, 589–590. (l) Prince, R. B.; Okada, T.; Moore, J. S. *Angew. Chem., Int. Ed. Engl.* **1999**, *38*, 233–236. (m) Appella, D. H.; Christianson, L. A.; Karle, I. L.; Powell, D. R.; Gellman, S. H. *J. Am. Chem. Soc.* **1999**, *121*, 6206–6212. (n) Appella, D. A.; Barchi, J. J.; Durell, S. R.; Gellman, S. H. *J. Am. Chem. Soc.* **1999**, *121*, 2309–2310. (o) Gung, B. W.; Zou, D.; Stalcup, A. M.; Cottrell, C. E. *J. Org. Chem.* **1999**, *64*, 2176–2177. (p) Appella, D. H.; Christianson, L. A.; Klein, D. A.; Richards, M. R.; Powell, D. R.; Gellman, S. H. *J. Am. Chem. Soc.* **1999**, *121*, 7574–7581.

The use of functionalized sugar scaffolds as peptide mimetics has also received some attention.^{2a,b,c,i,j,3} For example, in 1993, Hirschmann and co-workers demonstrated that an appropriately functionalized glucose residue could serve as a mimetic of a biologically active cyclic peptide.⁴ Hirschmann noted that monosaccharides are good scaffolds for the presentation of amino acid side chains because they can be derivatized easily, come in a variety of different stereoisomers, and have well-defined conformations, making it easy to predict the position of the functional groups. Oligosaccharides may make good scaffolds for mimicking larger elements of peptide structure because they too come in a wide variety of well-defined conformations and can be readily functionalized.⁵

In this paper, we present the synthesis and evaluation of a functionalized pentasaccharide **1** (Figure 1) that was designed to bind to duplex DNA. The design of the oligosaccharide scaffold and the development of an efficient synthetic route to the scaffold are described. The solution structure of the pentasaccharide has been determined by NMR and is consistent with the predicted structure. The functionalized oligosaccharide binds to DNA, and the mode of binding, determined by 2D NMR, shows that in several important respects the scaffold binds to DNA as designed.

Results and Discussion

Design. We have utilized structural motifs found in DNA binding proteins to design a DNA-binding oligosaccharide. Many proteins that bind to DNA utilize α helical recognition peptides. Most recognition helices are part of a larger folded

(3) Sofia, M. J.; Hunter, R.; Chan, T. Y.; Vaughan, A.; Dulina, R.; Wang, H.; Gange, D. *J. Org. Chem.* **1998**, *63*, 2802–2803.

(4) (a) Hirschman, R.; Nicolaou, K. C.; Pietranico, S.; Leahy, E. M.; Salvino, J.; Arison, B.; Cichy, M. A.; Spoons, P. G.; Shakespeare, W. C.; Sprengeler, P. A.; Hamley, P.; Smith, A. B., III; Reisine, T.; Raynor, K.; Maechler, L.; Donaldson, C.; Vale, W.; Friedinger, R. M.; Cascieri, M. R.; Strader, C. D. *J. Am. Chem. Soc.* **1993**, *115*, 12550–12568. (b) Hirschmann, R.; Haynes, J. J.; Cichy-Knight, M. A.; Van Rijn, R. D.; Sprengeler, P. A.; Spoons, P. G.; Shakespeare, W. C.; Pietranico-Cole, S.; Barbosa, J.; Liu, J.; Yao, W.; Rohrer, S.; Smith, A. B., III *J. Med. Chem.* **1998**, *41*, 1382–1391.

(5) Studies done with VSG proteins have shown that a trisaccharide can substitute for an α helix: Blum, M. L.; Down, J. A.; Gurnett, A. M.; Carrington, M.; Turner, M. J.; Wiley, D. C. *Nature* **1993**, *362*, 603–609.

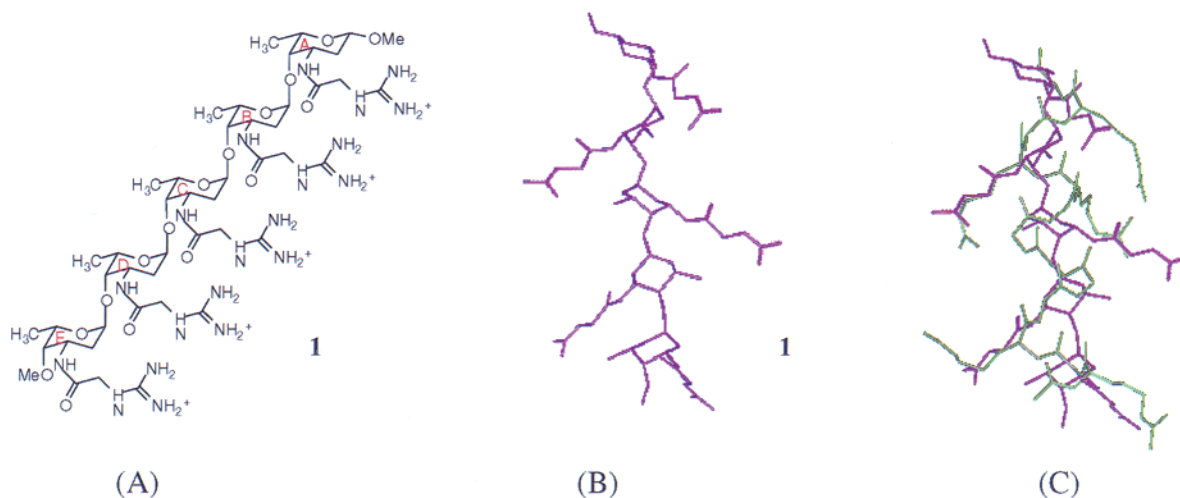


Figure 1. (A) The target pentasaccharide **1**. (B) The target pentasaccharide **1** shown in its preferred conformation. (C) Pentasaccharide **1** (purple) superimposed on residues 231–244 of GCN4 from a crystal structure of the DNA complex (green).⁷ Only arginine side chains within this region are shown.

unit that stabilizes the recognition helix while also making some contacts to the DNA. The basic regions of bZIP proteins, however, contact DNA as isolated helices that are not stabilized by tertiary contacts to other parts of the protein.⁶ Therefore, basic regions are the simplest type of recognition helices to try to mimic. Structural studies done with GCN4, a bZIP protein, have shown that it binds to DNA with one surface of the helix buried in the major groove.⁷ A number of arginine and lysine side chains emerge from the flanks of the helix and contact the phosphate backbone on both strands of the DNA duplex. The peptide backbone itself does not make any direct contacts to the DNA. In an abstract sense, a basic region peptide can be viewed as a cylinder from which positively charged groups emanate; the spacing between the charged groups is such that the helix can make at least two contacts to each strand of the phosphate backbone simultaneously.

With an idealized basic region helix as a blueprint for design, we searched for a rodlike oligosaccharide scaffold that could be easily functionalized to permit electrostatic contacts to both strands of the phosphate backbone. There is structural information showing that α -1,4-linked oligosaccharides display corresponding substituents on opposite sides of a central axis.⁸ We desired an oligosaccharide in which positive charges emerge from alternating sides of the molecule, a condition that appeared to be met in these oligosaccharides. A conformational analysis of α -1,4 glycosidic linkages shows that the conformation observed in X-ray structures and by NMR for this type of linkage is dictated by a combination of steric and electronic preferences.

Conformational Analysis. The overall shape of an oligosaccharide can be predicted by analyzing the low-energy conformations around the glycosidic linkages.⁹ In a glycosidic linkage to a secondary alcohol, there is free rotation around two bonds, the bond from the exocyclic oxygen to the anomeric carbon and the bond from the exocyclic oxygen to the carbon of the aglycone. The conformations around these two bonds are defined by two angles, ϕ and ψ , respectively. Sugars preferentially adopt

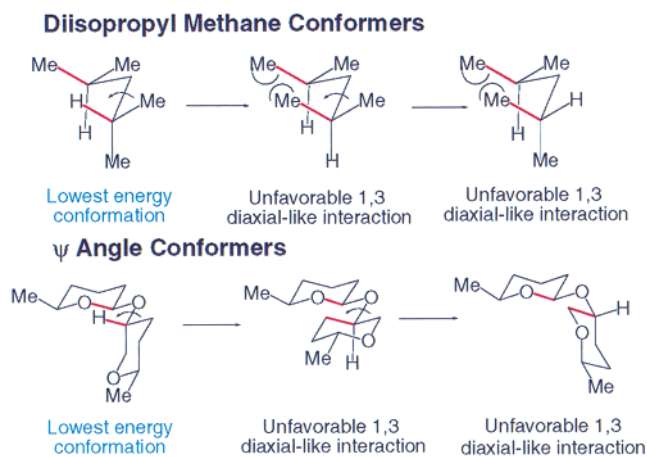


Figure 2. Steric analysis of ψ angle conformers showing analogous diisopropyl methane conformers.

conformations around the ϕ angle in which the lone pair of the exo oxygen is anti to the CO bond of the sugar ring (the so-called exo-anomeric effect). Only two of the three possible staggered conformations satisfy this criterion. For an equatorial glycosidic linkage, both conformers are populated to a significant extent. For axial glycosidic linkages, however, one of the two conformers is highly disfavored as a result of severe steric interactions. Therefore, axial glycosides adopt a single conformation around the ϕ angle. The preferred conformation around the ψ angle can be predicted by analyzing the nonbonded steric interactions. By holding the ϕ angle constant and rotating around the ψ angle, one can determine the conformation(s) that minimize unfavorable steric interactions (Figure 2). The nonbonded steric interactions that determine the preferred conformation for the nonanomeric C–O bond are analogous to those found in a diisopropylmethane unit. For example, just as is seen for diisopropylmethane, there is only one ψ angle conformer for the corresponding glycoside that does not have unfavorable 1,3-diaxial-like steric interactions.

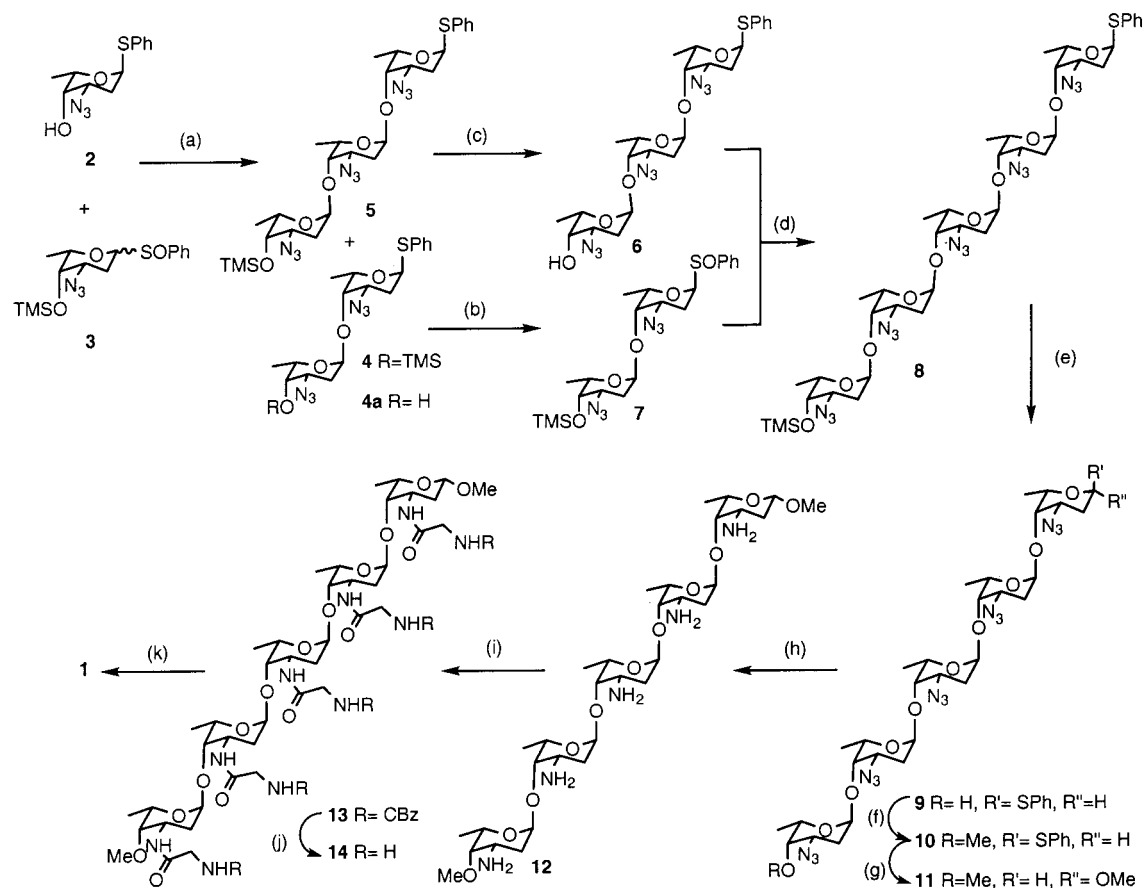
On the basis of the preceding analysis, we chose to make a homopolymer of α -1,4-linked fucose residues functionalized at C3 (**1**, Figure 1A). This α -1,4-homopolymer was predicted to have the rodlike conformation shown in Figure 1B. Molecular mechanics calculations also identify this structure as the low-energy conformation for **1**.¹⁰ Because of the preferred conformation around the glycosidic linkages, the C3 substituents on

(6) Hurst, H. C. *Protein Profile* **1994**, *1*, 123–168.

(7) Ellenberger, T. E.; Brandl, C. J.; Struhl, K.; Harrison, S. C. *Cell* **1992**, *71*, 1223–1237.

(8) (a) Faham, S.; Hileman, R. E.; Fromm, J. R.; Linhardt, R. J.; Rees, D. C. *Science* **1996**, *271*, 1116–1120. (b) The conformation of the trisaccharide portion of Aclacinomycin A is also consistent with this observation: Yang, D.; Wang, A. H. J. *Biochemistry* **1994**, *33*, 6595–6604.

(9) Lemieux, R. U.; Koto, S. *Tetrahedron* **1974**, *30*, 1933–1944.

Scheme 1. Synthesis of Pentasaccharide 1^a

^a Reaction conditions: (a) TiF_2O , 2,6-di-*tert*-butyl-4-methylpyridine, CH_2Cl_2 , -78°C , 44% of **4**, 9% of **4a**, 21% of **5**; (b) *m*CPBA, CH_2Cl_2 , -78°C , 85%; (c) HF·pyr/THF, 95%; (d) TiF_2O , 2,6-di-*tert*-butyl-4-methylpyridine, 4-allyl-3,4-dimethoxybenzene, CH_2Cl_2 , -78°C , 74%; (e) HF·pyr/THF, 90%; (f) (1) NaH, DMF and (2) CH_3I , DMF, 97%; (g) $\text{Hg}(\text{OCOCF}_3)_2$, MeOH, CH_2Cl_2 , 0°C (4:1 β : α), 94%; (h) H_2 , PtO_2 , MeOH, 90%; (i) H-Gly-NHCbz, HOBT, EDIC, DIEA, 85%; (j) H_2 , Pd/C, MeOH, 74%; (k) (1) CBzNHC(SMe)NCBz,³³ DMF, Et_3N , 45°C , 24 h, 85% and (2) H_2 , Pd/C, MeOH, 90%.

consecutive sugars are displayed from opposite sides of the scaffold. In **1**, these C3 substituents have been functionalized with guanidinium groups to mimic arginine side chains. Figure 1C shows an overlay of the low-energy conformation of pentasaccharide **1** and the GCN4 basic region helix from a crystal structure. There is reasonable correspondence between the position of the charged groups in the two structures.

It is worth making some additional points about the design of the oligosaccharide scaffold. 2-Deoxyfucose was chosen as a monomer building block because it is more hydrophobic than fully oxygenated sugars. The hydrophobicity was expected to help facilitate groove binding.^{11,12} An oligosaccharide composed of five monomers was chosen because the length is similar to that of the DNA binding portion of a basic region helix.

Synthesis of Pentasaccharide 1. One of the critical steps for the use of an oligosaccharide as a scaffold is the development of an efficient synthesis. Choosing a homopolymer as our initial target simplifies the synthesis of pentasaccharide **1** for two reasons. First, it is possible to obtain the requisite monomers **2** and **3** from a single precursor (Scheme 1). Second, it is possible to devise a highly convergent approach for coupling the monomers together. This approach involves the use of a polymerization reaction of the sulfoxide glycosylation method

to form disaccharide **4** and trisaccharide **5** in a single glycosylation reaction. Following isolation, these two components could then be coupled together to form a pentasaccharide using conditions which did not promote polymerization. Using this approach, only two glycosylation reactions would be required to assemble the pentasaccharide core **8**.

The synthetic strategy described above grew out of mechanistic investigations on the sulfoxide glycosylation reaction.^{13,14} We have identified conditions to permit multiple glycosylation reactions to occur to form a mixture of products of different lengths. Mechanistic studies in this laboratory have shown that there are two pathways in which an acceptor such as **2**, which contains an anomeric sulfide, and a sulfoxide donor such as **3** can react to give products longer than a disaccharide (Scheme 1). One way involves the loss of the TMS group on the donor during the reaction to expose an acceptor site that can react with another molecule of donor. The other way involves activation of the anomeric sulfide at the reducing end of the glycosyl acceptor by phenyl sulfenyl triflate, which is generated during the course of the sulfoxide reaction. Both of these processes work to our advantage in the first glycosylation reaction, in which we want to obtain both di- and trisaccharide

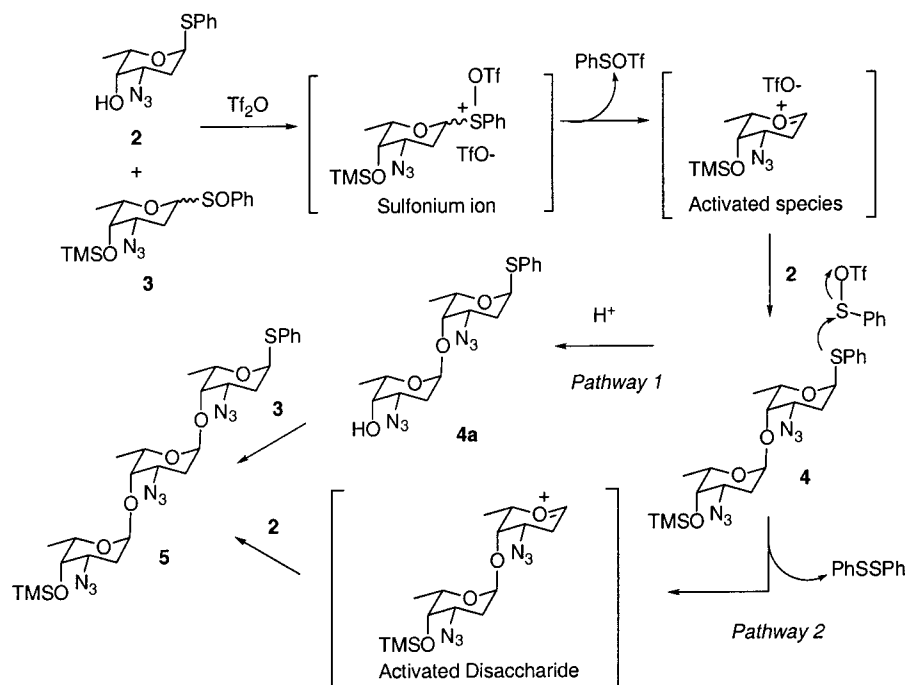
(10) Molecular modeling studies were done on pentasaccharide **1** using published methods, see: Senderowitz, H.; Parish, C.; Still, W. C. *J. Am. Chem. Soc.* **1996**, *118*, 2078–2086.

(11) Kahne, D. *Chem., Biol.* **1995**, *2*, 7–12.

(12) Ding, W.; Ellestad, G. A. *J. Am. Chem. Soc.* **1991**, *113*, 6617–6620.

(13) (a) Raghavan, S.; Kahne, D. *J. Am. Chem. Soc.* **1993**, *115*, 1580–1581. (b) Gildersleeve, J.; Pascal, R. A.; Kahne, D. *J. Am. Chem. Soc.* **1998**, *120*, 5961–5969. (c) Gildersleeve, J.; Smith, A.; Sakurai, K.; Raghavan, S.; Kahne, D. *J. Am. Chem. Soc.* **1999**, *121*, 6176–6182.

(14) For other mechanistic studies on the sulfoxide reaction, see: (a) Crich, D.; Sun, S. *J. Am. Chem. Soc.* **1997**, *119*, 11217–11223. (b) Crich, D.; Sun, S. *J. Am. Chem. Soc.* **1998**, *120*, 435–436.

Scheme 2. Potential Mechanisms for Trisaccharide **5** Formation

products. However, it is important to suppress processes that lead to polymerization in the second glycosylation reaction to ensure that only pentasaccharide is formed. We have identified conditions to suppress unwanted activation of anomeric sulfides during glycosylations using anomeric sulfoxide donors. Hence, as described below, our synthesis involved two successive glycosylation reactions run under different conditions (Scheme 1).

Monomer **2** was prepared from commercially available rhamnose.¹⁵ Monomer **3** was synthesized from **2** via silylation and oxidation. The monomers were then coupled under conditions that permit sulfide activation to form **4** and **5** in a combined yield of 65%. Disaccharide **4** and trisaccharide **5** were converted to the requisite donor disaccharide **7** and acceptor trisaccharide **6**, respectively, as shown in Scheme 1. The glycosylation reaction was carried out using the inverse addition procedure, which involves the slow addition of sulfoxide to a pre-cooled solution of acceptor, triflic anhydride, and base. This inverse addition method of activation prevents anomeric sulfenation formation, which is a facile side reaction with activated 2-deoxy donors. Trisaccharide **6** and disaccharide **7** were then coupled to form pentasaccharide **8**. The sulfoxide glycosylation conditions in this case included the addition of a phenyl sulfonyl triflate scavenger to suppress sulfide activation and prevent the formation of undesired higher order oligomers. The pentasaccharide was produced in 74% yield as a single stereoisomer, and no higher order oligomers were detected.¹⁶ Using this approach, the pentasaccharide core was obtained rapidly and efficiently in an overall yield of 26% from monomers **2** and **3**.

(15) Compounds **2** and **3** were synthesized from readily available 2-deoxy-3-azido-4-O-acetyl-L-rhamnopyranoside (Florent, J. F.; Monneret, C. *J. Chem. Soc., Chem. Commun.* **1987**, 1171–1172). (1) Ac₂O, pyridine, DMAP, room temperature, 20 min; (2) PhSH, BF₃·Et₂O, CH₂Cl₂, 20 min, room temperature, 93% over two steps; (3) K₂CO₃, MeOH, room temperature, 2 h; (4) Tf₂O, pyridine, CH₂Cl₂, 1 h, 75% over two steps; (5) KOBz, 18-crown-6, DMF, 4 h; (6) LiOH, MeOH, 99% over two steps to give **2**; (7) TMSOTf, TEA, CH₂Cl₂, -78 °C, 20 min; (8) mCPBA, CH₂Cl₂, -42 °C, 92% over two steps to give **3**. For experimental details, see: Smith, A. Ph.D. Thesis, Princeton University, 1997.

(16) This result suggests that the primary pathway for polymerization of these substrates involves activation of the anomeric sulfide with phenylsulfonyl triflate (Pathway 2, Scheme 2).

Table 1. ¹H Chemical Shifts (ppm) of the Nonexchangeable Pentasaccharide Resonances in the Free Pentasaccharide **1** (Chemical Shift Differences are also Reported for Pentasaccharide **1** in the Pentasaccharide **1**-d[GGAATTC] Complex³⁵)

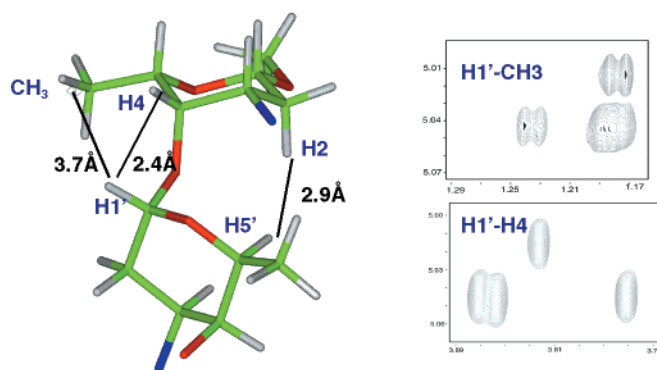
	A	B, C, D ³⁵	E
H1	4.61(+0.01)	5.04(+0.01)	5.01(+0.03)
H2ax	1.64(+0.02)	2.02–2.03(+0.01)	1.89(+0.02)
H2eq	1.84(+0.02)	1.86–1.88(+0.01)	1.84(+0.02)
H3	4.04(+0.02)	4.32–4.33(+0.01)	4.35(+0.02)
H4	3.76(+0.01)	3.83(+0.01), 3.87–3.88(+0.01)	3.41(+0.02)
H5	3.76(+0.01)	4.22–4.23(+0.02)	4.19(+0.02)
CH ₃	1.23(+0.02)	1.17–1.18(+0.02)	1.20(+0.02)
OCH ₃	3.47(-0.04)		3.48(+0.02)

The final stage of the synthesis of the target pentasaccharide involved the installation of the guanidinium groups. This was effected by simultaneously reducing the five azides to give the pentamine **12**. The amines were reacted with the activated glycine derivative followed by removal of the protecting groups to generate **14**. In the final stage, the guanidine moiety was installed to provide **1**. The synthesis of pentasaccharide **1** is versatile and efficient, allowing for many analogues with different functionality to be made and tested.

Solution Conformation of 1. With the pentasaccharide in hand, we conducted a series of NMR experiments to determine whether **1** adopts the predicted conformation in solution. The nonexchangeable proton resonances in D₂O were assigned using a combination of 2Q-HoMQC, TOCSY, ROESY, and NOESY experiments. Assignments were readily made for the terminal sugars (A and E). Assignments were slightly more difficult for the internal sugars (B, C, and D) due to overlap of some of the resonances. However, the individual spin systems could be assigned and the chemical shifts of at least some of the protons were sufficiently different to permit sequence-specific assignments to be made (Table 1). Interresidue NOE cross-peaks between CH₃ and H1', H4 and H1', and H2 and H5' were observed around all four glycosidic linkages as shown in Figure 3. These NOEs are consistent with the predicted glycosidic linkage conformation shown in Figure 1B.

Table 2. Energetics of DNA Binding for (A) Pentasaccharide **1** and (B) Pentalysine

[Na ⁺] (M)	K _d (obs) (M ⁻¹)	ΔG(obs) (kcal/mol)	ΔG _{pe} (kcal/mol)	ΔG _T (kcal/mol)
(A) pentasaccharide 1				
0.015	3.0 × 10 ⁶	-8.83	-6.59	-2.24
0.040	2.1 × 10 ⁵	-7.25	-5.05	-2.20
0.090	2.6 × 10 ⁴	-6.01	-3.78	-2.23
(B) pentalysine				
0.015	5.8 × 10 ⁵	-7.85	-6.59	-1.27
0.040	5.1 × 10 ⁴	-6.41	-5.05	-1.37
0.090	5.0 × 10 ³	-5.04	-3.78	-1.26

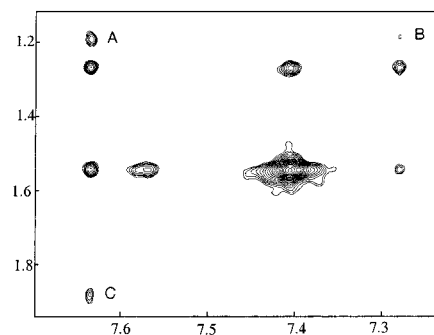
**Figure 3.** (A) The estimated distances corresponding to NOE cross-peaks observed between H1' and CH₃, H1' and H4, and H5' and H2. These distances were consistent with the preferred conformation of **1** shown in Figure 1B. (B) Interresidue cross-peaks between H1' and CH₃, and H1' and H4.

DNA Binding. As a preliminary evaluation of the pentasaccharide, the DNA binding properties were measured using an ethidium bromide assay.¹⁷ The pentasaccharide was found to bind to calf thymus DNA with a dissociation constant of ~10⁻⁶ M. Virtually all positively charged compounds interact with DNA under appropriate conditions, and the estimated affinity of the pentasaccharide is only slightly higher than that of pentalysine, a flexible peptide containing the same net charge. Pentalysine binds to DNA almost entirely by electrostatic interactions. To determine whether the binding of pentasaccharide **1** is also due primarily to electrostatic interactions, we measured the salt dependence of the binding constant.¹⁸ The results show that the polyelectrolyte contribution (ΔG_{pe}) to binding is virtually identical for both pentasaccharide **1** and pentalysine (Table 2). However, the nonpolyelectrolyte contribution to binding (ΔG_T) is 1 kcal/mol higher for pentasaccharide **1** than for pentalysine. Hence, the increase in binding affinity for pentasaccharide **1** relative to pentalysine is due to something other than electrostatic interactions.

The next step was to try to determine if pentasaccharide **1** discriminates between duplex DNA and other types of nucleic acids. To address this question, we investigated the ability of **1** to displace ethidium bromide from yeast RNA.¹⁹ RNA also has a negatively charged phosphate backbone and double stranded regions, like DNA. The conformation of an RNA duplex, however, is quite different from the conformation of a typical B form DNA duplex. For example, an RNA duplex has a wider and shallower minor groove and contains phosphates that are spaced differently than in a DNA duplex. The assay results showed that pentasaccharide **1** did not displace ethidium from

(17) LePecq, J. B.; Paoletti, C. *J. Mol. Biol.* **1967**, *27*, 87–106.(18) Chaires, J. B. *Anti-Cancer Drug Des.* **1996**, 569–580.(19) Sakai, T. T.; Torget, R.; I, J.; Freda, C. E.; Cohen, S. S. *Nucleic Acids Res.* **1975**, *2*, 1005–1022.**Table 3.** ¹H Chemical Shifts (ppm) of the Nonexchangeable DNA Resonances in the Free DNA and the Pentasaccharide **1**-d[GGAATTCC]₂ Complex

	H8/H6	H5	H2	CH ₃	H1'
G1	7.80(+0.01)				5.55(+0.03)
G2	7.80(+0.01)				5.40(0.00)
A3	8.15(+0.02)		7.26(+0.02)		6.01(+0.02)
A4	8.15(+0.02)		7.62(+0.01)		6.18(+0.01)
T5	7.14(+0.01)			1.24(+0.03)	5.94(0.00)
T6	7.14(+0.01)			1.52(+0.02)	6.12(0.00)
C7	7.56(+0.01)	5.67(+0.01)			6.01(-0.01)
C8	7.62(-0.02)	5.75(-0.05)			6.21(0.00)

**Figure 4.** NOESY cross-peaks between (A) A4H2 and a hexose methyl, (B) A3H2 and a hexose methyl, and (C) A4H2 and a hexose H2'/H2'' pair.

double stranded regions of yeast tRNA even at concentrations 2-fold higher than were used to displace ethidium from duplex DNA.

These preliminary studies indicated that pentasaccharide **1** discriminates between duplex DNA and duplex RNA, raising the possibility that there might be a specific binding mode. Consequently, we undertook an investigation of DNA binding using NMR. A 0.5:1 and 1:1 complex of the pentasaccharide and the self-complementary DNA duplex d-(G₁G₂A₃A₄T₅T₆C₇C₈)₂ were prepared in buffered water.^{20,21} There were small chemical shift differences between the free DNA and pentasaccharide controls and the 1:1 complex, consistent with an interaction between the DNA and **1** (Tables 1 and 3). A single set of resonance lines were observed for the 0.5:1 pentasaccharide/DNA complex, indicating that the ligand is in fast exchange between the free and bound states.

The NOESY spectra of the 1:1 complex confirms that the pentasaccharide binds to DNA and also provides evidence about the mode of binding. Although the ligand is in fast exchange, we were able to identify several intermolecular NOEs. The strongest resolved NOE cross-peaks were between the adenine H2 protons and two of the pentasaccharide methyl groups as well as one pair of 2-deoxy protons (Figure 4). All three of these groups of protons were assigned to the internal sugars in the pentasaccharide. Although sequence-specific assignments for the three internal sugars in the complex could not be made with certainty, only one set of assignments can account for these NOEs. In the low-energy conformation of the pentasaccharide, the C5 methyl groups of residues B and D, and the 2-deoxy protons on residue C are located on the same side of the

(20) This DNA sequence has been well-characterized by NMR: (a) Patel, D. J. *Eur. J. Biochem.* **1979**, *99*, 369–378. (b) Patel, D. J.; Canuel, L. L. *Eur. J. Biochem.* **1979**, *96*, 267–276. (c) Broido, M. S.; Zon, G.; James, T. L. *Biochem. Biophys. Res. Commun.* **1984**, *119*, 663–670.(21) An internally AT-rich DNA sequence was chosen since it has been shown that arginine residues in peptides prefer AT regions in DNA: Geierstanger, B. H.; Volkman, B. F.; Kremer, W.; Wemmer, D. E. *Biochemistry* **1994**, *33*, 5347–5355.

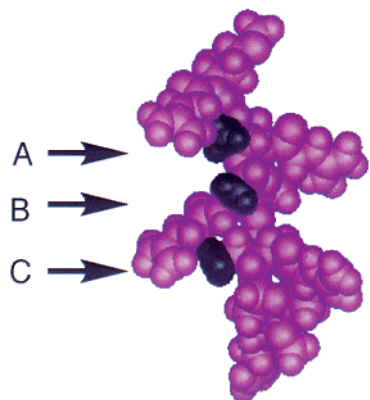


Figure 5. Pentasaccharide **1** highlighting the hydrophobic contacts made to DNA in the minor groove by (A) the C5 methyl group on residue B, (B) the 2-deoxy protons on residue C, and (C) the C5 methyl group on residue D.

molecule, creating a hydrophobic cluster (Figure 5). The same interresidue NOEs are observed in the pentasaccharide in the absence and presence of DNA, suggesting that the conformation of the oligosaccharide does not change upon binding to DNA. Therefore, we infer that the face of the pentasaccharide containing the hydrophobic cluster, formed by methyl protons on residues B and D and the H₂ protons on residue C, is buried in the minor groove giving rise to the observed NOESY cross-peaks to the adenine H2 protons. It is worth noting that when the oligosaccharide is docked into the minor groove with the NOESY contacts satisfied, the basic side chains on the pentasaccharide are positioned to contact both strands of the DNA duplex, as designed.

Conclusion

We have designed a groove binding oligosaccharide that interacts with duplex DNA. Based on a self-consistent set of NOEs, we have shown that the oligosaccharide binds to DNA in the minor groove with one surface of the oligosaccharide contacting the floor of the DNA. The major driving force for binding involves electrostatic contacts. Nevertheless, the molecule is able to discriminate between duplex DNA and duplex RNA, showing that it has shape selectivity. Pentasaccharide **1** differs from the basic region helices that inspired its design in that it binds in the minor groove rather than the major groove. It is possible that the preference for major or minor groove binding is related to the dimensions of the molecules. Basic region peptides are larger in diameter than the functionalized oligosaccharide. If so, it might be possible to facilitate a switch in grooves by increasing the size of some of the substituents. It may also be possible to manipulate sequence selectivity by altering the groups that point in toward the floor of the groove.

Experimental Section

Synthesis of Pentasaccharide 1. One-dimensional NMR spectra were recorded on a Varian UNITY/Inova 500-MHz Fourier transform NMR spectrometer. Chemical shifts (δ) are reported in parts per million (ppm) downfield from tetramethylsilane (TMS) unless otherwise noted. Coupling constants (J) are reported in hertz (Hz). Multiplicities are abbreviated as follows: singlet (s), doublet (d), triplet (t), quartet (q), multiplet (m), and broadened (br). Mass spectra were obtained on a VG ZAB, VG 7070, HP 5989A (University of California, Riverside, Mass Spectrometry Facility).

Analytical thin-layer chromatography (TLC) was performed using silica gel 60 F254 precoated plates (0.25 mm thickness) with a fluorescent indicator. Flash column chromatography was performed

using silica gel 60 (230–400 mesh) from EM Science/Bodman. CM-Sephadex ion-exchange resin was purchased from Sigma.

All reactions were carried out under argon atmosphere with dry, freshly distilled solvents under anhydrous conditions unless otherwise noted. All reagents were purchased from commercial suppliers and used without further purification unless otherwise noted.

DNA and RNA Binding Assay. Sonicated calf thymus DNA was purchased from Pharmacia Biotech. Yeast-soluble RNA was obtained from Calbiochem. An absorbance was measured and the concentration of RNA was determined using a millimolar extinction coefficient of 570 mM⁻¹ cm⁻¹ at 260 nm.²² DNA binding was conducted at 15 mM NaCl, 25 mM Tris, pH 7.5. RNA binding was conducted at 50 mM KCl, 50 mM potassium cacodylate, pH 7.0. Fluorescence measurements were made using a Perkin-Elmer LS 50 fluorescence spectrophotometer.

Binding constants were determined by carrying out fluorescence titrations in which calf thymus DNA or yeast RNA concentrations were fixed at 1 μ M each. Stock solutions of pentasaccharide **1** were made in the respective buffer for titration. The excitation wavelength for DNA studies was set to 546 nm and all emitted light passing through a 600 nm cutoff filter was collected. For RNA, the excitation wavelength was set to 520 nm and all emitted light passing through a 590 nm cutoff filter was collected. All titrations were carried out at 25 °C. The salt dependence of the equilibrium binding constant ($K_a(\text{obs})$) was determined using the same DNA binding buffer at 15, 40, and 90 mM NaCl. Fluorescence titrations were directly fit to obtain binding constants using Kaleidagraph (Synergy Software, Reading, PA).

NMR. Purified DNA was synthesized on a 10 μ mol scale at the Princeton Synthesis Facility. Following dialysis to remove TEA salts, the strands were lyophilized and dissolved in 1 mL of NMR buffer (25 mM phosphate, pH 7). An absorbance was measured and the concentration was determined from the calculated extinction coefficient at 260 nm (54×10^3 M⁻¹ cm⁻¹).²³ After annealing and repeated lyophilization from D₂O, a sample was prepared containing 2.4 mM of the DNA duplex in 0.5 mL of D₂O. A 0.5 or 1.0 equiv sample of pentasaccharide **1** in 100 μ L of D₂O was added to the DNA. The sample was lyophilized and redissolved in 0.5 mL of D₂O. No precipitate was observed.

All one-dimensional and two-dimensional NMR experiments were run on a Varian Unity/INOVA NMR spectrometer at 600 MHz and at 10 °C, unless indicated otherwise. Through bond connectivities were mapped by gradient-selected 2Q-HoMQC²⁴ and TOCSY using a z-filtered MLEV-16 based spin-lock period,²⁵ while ROESY²⁵ and NOESY²⁶ were used to determine through space interactions. The water signal in H₂O samples was suppressed using the WATERGATE method²⁷ with selective pulses of 1.7 ms. For 2D experiments in H₂O additional gradient pulses were applied during the t_1 incremented delay and for most of the NOESY mixing time to suppress radiation damping.²⁸ Typical 2D acquisition parameters include a 8 kHz spectral window in both dimensions, t_1^{max} of 64–100 ms, 16–32 scans for each increment, and States-Redfield sign discrimination²⁹ in the remote dimension.

One-dimensional spectra were processed by the Vnmr software (Varian, Inc., Palo Alto, CA). All 2D spectra were processed off-line with NMRPipe³⁰ using standard procedures,²⁹ and subsequently visualized and analyzed in NMRView.³¹ Typical 2D processing parameters

(22) Lindahl, T.; Henley, D. D.; Fresco, J. R. *J. Am. Chem. Soc.* **1965**, *87*, 4961–4963.

(23) Patel, D. J.; Canuel, L. L. *Eur. J. Biochem.* **1979**, *96*, 267–276.

(24) Pelczer, I.; Bishop, K. D. *Methods for Structure Elucidation by High-Resolution NMR*; Kover, K. E., Batta, G., Szantay, J. Cs., Eds.; Elsevier: 1997; pp 187–207.

(25) (a) Rance, M. *J. Magn. Reson.* **1987**, *74*, 557–564. (b) Bax, A. *Isr. J. Chem.* **1988**, 309–317.

(26) Neuhaus, D.; Williamson, M. P. *The Nuclear Overhauser Effect in Structural and Conformational Analysis*; VCH Publishers: New York, 1987.

(27) Piotto, M.; Saudek, V.; Sklenar, V. *J. Biomol. NMR* **1992**, *2*, 661–666.

(28) Sklenar, V. *J. Magn. Reson., Ser. A* **1995**, *114*, 132–135.

(29) Pelczer, I.; Carter, B. G. *Methods in Molecular Biology*; Reid, D. G., Eds.; Humana Press: Totowa, NJ, 1997; pp 71–156.

(30) Delaglio, F.; Grzesiek, S.; Vuister, G. W.; Zhu, G.; Pfeifer, J.; Bax, A. *J. Biomol. NMR* **1995**, *6*, 277–293.

(31) Johnson, B. A.; Blevins, R. A. *J. Biomol. NMR* **1994**, *4*, 603–614.

were as follows: time domain filtering of the residual solvent signal if necessary, apodization with a slightly shifted cosine function in combination with additional Gaussian broadening in both dimensions, removal of the axial peaks using time domain filtering again, baseline correction with 4th-order polynomial as necessary, and zero filling in both dimensions. Final size of the frequency domain spectra was 8K × 2K data points.

Phenyl (3-Azido-2,3-dideoxy-4-trimethylsilyl- α -L-fucopyranosyl)-(1-4)-3-azido-2,3-dideoxy-1-thio- α -L-fucopyranoside (4). Alcohol **2** (518 mg, 1.95 mmol) and 2,6-di-*tert*-butyl-4-methylpyridine (1.06 g, 5.2 mmol) were combined and residual water was removed by azeotropic distillation with toluene (3 × 20 mL). To the residue in methylene chloride (26 mL) was added 4 Å molecular sieves (500 mg), and the resulting suspension was stirred at room temperature. The suspension was cooled to -78 °C, and triflic anhydride (219 μ L, 1.3 mmol) was added over 1–2 min. A solution of sulfoxide **3** (460 mg, 1.3 mmol) in methylene chloride (17 mL) was added via syringe over 10–15 min. After 15 min at -78 °C, the reaction was quenched with diethylamine (1 mL), filtered into saturated aqueous NaHCO₃ (100 mL), and extracted with methylene chloride (3 × 80 mL). The organic layers were combined, dried over Na₂SO₄, filtered, and concentrated in vacuo. The product was purified by flash chromatography (10% EtOAc/petroleum ether) to afford disaccharide **4** (280 mg, 44%): *R*_f = 0.44 (10% EtOAc/petroleum ether); ¹H NMR (CDCl₃) δ 7.47–7.46 (m, 2H), 7.32–7.24 (m, 3H), 5.71 (d, *J* = 5.5 Hz, 1H), 5.08 (d, *J* = 3.1 Hz, 1H), 4.33 (q, *J* = 6.4 Hz, 1H), 4.25 (q, *J* = 6.4 Hz, 1H), 3.96 (ddd, *J* = 12.21, 3.7, 3.36 Hz, 2 H), 3.80–3.68 (m, 2H), 2.38 (ddd, *J* = 13.0, 13.0, 5.8, 1H), 2.22 (ddd, *J* = 12.5, 12.5, 3.7 Hz, 1H), 2.05–1.97 (m, 2H), 1.23 (d, *J* = 6.7 Hz, 3H), 1.21 (d, *J* = 6.4 Hz, 3H), 0.22 (2, 3H); ¹³C NMR (CDCl₃, 125.8 MHz) δ 134.6, 131.1, 129.0, 127.2, 98.8, 83.5, 75.1, 71.1, 67.8, 67.7, 58.0, 56.6, 30.8, 28.2, 17.7, 17.4, 0.5; HRFABMS calcd for C₂₁H₃₂O₄N₆SSi (M + Na⁺) 515.1873, found 515.1891.

Phenyl (3-Azido-2,3-dideoxy- α -L-fucopyranosyl)-(1-4)-3-azido-2,3-dideoxy-1-thio- α -L-fucopyranoside (4a) (49 mg, 9%): *R*_f = 0.17 (20% EtOAc/petroleum ether); ¹H NMR (CDCl₃) δ 7.46–7.44 (m, 2H), 7.32–7.25 (m, 3H), 5.69 (d, *J* = 5.2 Hz, 1H), 5.04 (d, *J* = 2.6 Hz, 1H), 4.34 (q, *J* = 6.3 Hz, 2H), 3.96 (ddd, *J* = 9.7, 4.2, 3.3 Hz, 2H), 3.84–3.71 (m, 2H), 2.37 (ddd, *J* = 13.0, 13.0, 5.8 Hz, 1H), 2.15–2.01 (m, 3H), 1.29 (d, *J* = 6.7 Hz, 3H), 1.23 (d, *J* = 6.7 Hz, 3H); ¹³C NMR (CDCl₃, 125.8 MHz) δ 134.6, 131.3, 129.2, 127.5, 99.0, 83.7, 75.7, 69.9, 67.7, 67.2, 58.1, 57.0, 30.9, 28.7, 17.5, 17.2; HRFABMS calcd for C₂₁H₂₄O₄N₆S (M + Na⁺) 443.1477, found 443.1497.

Phenyl [(3-Azido-2,3-dideoxy-4-trimethylsilyl- α -L-fucopyranosyl)-(1-4)-(3-azido-2,3-dideoxy- α -L-fucopyranosyl)]-(1-4)-3-azido-2,3-dideoxy-1-thio- α -L-fucopyranoside (5) (90 mg, 21%): *R*_f = 0.30 (10% EtOAc/petroleum ether); ¹H NMR (CDCl₃) δ 7.45–7.44 (m, 2H), 7.32–7.24 (m, 3H), 5.70 (d, *J* = 5.2 Hz, 1H), 5.06 (d, *J* = 16.5 Hz, 2H), 4.34 (q, *J* = 6.6 Hz, 1H), 4.29 (q, *J* = 6.5 Hz, 1H), 4.24 (q, *J* = 6.3 Hz, 1H), 4.00–3.96 (m, 3H), 3.80–3.67 (m, 3H), 2.37 (ddd, *J* = 13.1, 13.0, 5.5 Hz, 1H), 2.20 (ddd, *J* = 12.5, 12.5, 3.4 Hz, 1H), 2.05–1.97 (m, 4H), 1.24 (d, *J* = 6.7 Hz, 3H), 1.22 (d, *J* = 6.7 Hz, 3H), 1.18 (d, *J* = 6.4 Hz, 3H), 0.19 (s, 9H); ¹³C NMR (CDCl₃, 125.8 MHz) δ 134.6, 131.3, 129.2, 127.4, 98.9, 98.8, 83.7, 75.4, 75.2, 71.3, 67.9, 67.8, 67.7, 58.1, 56.9, 56.8, 30.9, 29.8, 28.3, 17.8, 17.7, 17.5, 0.6; HRFABMS calcd for C₂₇H₄₁O₆N₉SSi (M + Na⁺) 670.2567, found 670.2557.

Phenyl [(3-Azido-2,3-dideoxy- α -L-fucopyranosyl)]-(1-4)-(3-azido-2,3-dideoxy- α -L-fucopyranosyl)]-(1-4)-3-azido-2,3-dideoxy-1-thio- α -L-fucopyranoside (6). A solution (1.5 mL) of freshly prepared, buffered pyridinium hydrofluoride (10 mL of THF, 5.7 mL of pyridine, and 2.1 g of pyridinium hydrofluoride)³² was added to a plastic vial containing **5** (90 mg, 0.139 mmol) in THF (1.5 mL). The reaction was quenched after 0.5 h with 5 mL of saturated aqueous NaHCO₃. The aqueous layer was extracted with methylene chloride (3 × 5 mL), and the organic layers were combined, dried over Na₂SO₄, concentrated in vacuo, and purified by flash chromatography (20% EtOAc/petroleum ether) to give 76 mg (95%) of **6**: *R*_f = 0.14 (20% EtOAc/petroleum ether); ¹H NMR (CDCl₃) δ 7.45–7.44 (m, 2H), 7.32–7.24 (m, 3H), 5.70 (d, *J* = 5.5 Hz, 1H), 5.05 (s, 2H), 4.40–4.29 (m, 3H), 4.03–3.96

(m, 2H), 3.86–3.71 (m, 4H), 2.41–2.33 (m, 2H), 2.14–1.96 (m, 4H), 1.37–1.20 (m, 9H); ¹³C NMR (CDCl₃, 125.8 MHz) δ 134.6, 131.3, 129.2, 127.5, 98.9, 83.7, 75.8, 75.5, 70.0, 67.9, 67.7, 67.1, 58.2, 57.1, 56.9, 30.9, 29.9, 28.7, 17.7, 17.6, 17.0; HRFABMS calcd for C₂₄H₃₃O₆N₉S (M + Na⁺) 598.2172, found 598.2204.

Phenyl [(((3-Azido-2,3-dideoxy-4-trimethylsilyl- α -L-fucopyranosyl)]-(1-4)-(3-azido-2,3-dideoxy- α -L-fucopyranosyl)]-(1-4)-(3-azido-2,3-dideoxy- α -L-fucopyranosyl)]-(1-4)-(3-azido-2,3-dideoxy-1-thio- α -L-fucopyranoside (8). To disaccharide **4** (150 mg, 0.30 mmol) in methylene chloride (6 mL) at -42 °C was added 3-chloroperoxybenzoic acid (114 mg of 65% dispersion, 1.03 mmol). The reaction was allowed to warm to -20 °C, and dimethyl sulfide (30 μ L) was added. The reaction was diluted with methylene chloride (15 mL) and extracted with saturated aqueous NaHCO₃ (2 × 15 mL). The organic layer was dried over Na₂SO₄ and concentrated in vacuo. The products were purified by flash chromatography (35% EtOAc/petroleum ether) to afford **7** (128 mg, 85%).

Alcohol **6** (73 mg, 0.127 mmol), 4-allyl-1,2-dimethoxybenzene (218 μ L, 1.27 mmol), and 2,6-di-*tert*-butyl-4-methylpyridine (130 mg, 0.63 mmol) were combined, and residual water was removed by azeotropic distillation with toluene (3 × 10 mL). To the residue in methylene chloride (2.3 mL) and diethyl ether (2.3 mL) was added 4 Å molecular sieves (500 mg), and the resulting suspension was stirred at room temperature. The suspension was cooled to -78 °C, and triflic anhydride was added (43 μ L, 0.25 mmol) over 1–2 min. A solution of sulfoxide **7** (128 mg, 0.25 mmol) in methylene chloride (1 mL) was added via syringe over 10–15 min. After 15 min at -78 °C, the reaction was quenched with diethylamine (150 μ L), filtered into saturated aqueous NaHCO₃ (45 mL), and extracted with methylene chloride (3 × 35 mL). The organic layers were combined, dried over Na₂SO₄, filtered, and concentrated in vacuo. The product was purified by flash chromatography (20% EtOAc/petroleum ether) to afford pentasaccharide **8** (90 mg, 74%): *R*_f = 0.41 (20% EtOAc/petroleum ether); ¹H NMR (CDCl₃) δ 7.45–7.44 (m, 2H), 7.32–7.25 (m, 3H), 5.71–5.70 (d, *J* = 5.5 Hz, 1H), 5.08–5.05 (m, 4H), 4.35–4.23 (m, 5H), 4.01–3.96 (m, 5H), 3.77–3.67 (m, 5H), 2.36 (ddd, *J* = 12.9, 12.8, 5.5 Hz, 1H), 2.20 (ddd, *J* = 12.4, 12.4, 3.7 Hz, 1H), 2.04–1.97 (m, 8H), 1.29–1.18 (m, 15 H), 0.19 (s, 9H); ¹³C NMR (CDCl₃, 125.8 MHz) δ 134.6, 131.3, 129.2, 127.5, 98.9, 98.8, 98.7, 83.7, 75.5, 75.3, 71.3, 67.8, 67.7, 60.6, 58.1, 57.0, 56.8, 30.9, 29.8, 28.3, 21.2, 17.8, 17.7, 17.5, 14.4, 0.6; HRFABMS calcd for C₃₉H₅₉O₁₀N₁₅SSi (M + Na⁺) 980.3957, found 980.3951.

Methyl [(((3-Azido-2,3-dideoxy-4-*O*-methyl- α -L-fucopyranosyl)]-(1-4)-(3-azido-2,3-dideoxy- α -L-fucopyranosyl)]-(1-4)-(3-azido-2,3-dideoxy- α -L-fucopyranosyl)]-(1-4)-3-azido-2,3-dideoxy- α -L-fucopyranoside (11). A solution (1.4 mL) of freshly prepared, buffered pyridinium hydrofluoride (10 mL of THF, 5.7 mL of pyridine, and 2.1 g of pyridinium hydrofluoride)³² was added to a plastic vial containing **8** (90 mg, 0.094 mmol) in THF (3 mL). The reaction was quenched after 1 h with 5 mL of saturated aqueous NaHCO₃. The aqueous layer was extracted with methylene chloride (3 × 5 mL), and the organic layers were combined, dried over Na₂SO₄, concentrated in vacuo, and purified by flash chromatography (10% MeOH/CHCl₃) to give 75 mg (90%) of **9**: *R*_f = 0.31 (10% MeOH/CHCl₃); ¹H NMR (CDCl₃) δ 7.45–7.44 (m, 2H), 7.32–7.24 (m, 3H), 5.70 (d, *J* = 5.5 Hz, 1H), 5.05 (s, 4H), 4.37–4.29 (m, 5H), 4.02–3.97 (m, 5H), 3.82–3.71 (m, 5H), 2.37 (ddd, *J* = 13.1, 13.0, 5.5 Hz, 1H), 2.14–1.98 (m, 9H), 1.28 (d, *J* = 6.7 Hz, 3H), 1.27–1.22 (m, 12 H); ¹³C NMR (CDCl₃, 125.8 MHz) δ 134.6, 131.3, 129.2, 127.4, 98.8, 98.7, 83.6, 75.8, 75.5, 70.0, 67.8, 67.7, 67.6, 67.1, 60.6, 58.1, 57.0, 56.9, 30.9, 29.8, 28.7, 21.2, 17.7, 17.5, 17.0, 14.4; HRFABMS calcd for C₃₆H₅₁O₁₀N₁₅S (M + Na⁺) 908.3562, found 908.3610.

To a solution of **9** (75 mg, 0.085 mmol) in DMF (1.5 mL) was added sodium hydride (4 mg of 95% in mineral oil, 0.127 mmol). The mixture was allowed to stir for 5 min before addition of methyl iodide (11 μ L, 169 μ mol). After 20 min of stirring, the mixture was diluted with methylene chloride and poured into saturated aqueous NaHCO₃. The organic layer was washed with saturated aqueous NaHCO₃ (2 × 10 mL), dried over Na₂SO₄, concentrated, and purified by flash chromatography (20% EtOAc/petroleum ether) to afford **10** (76 mg, 97%). *R*_f

(32) Trost, B. M.; Caldwell, C. G.; Murayama, E.; Heissler, D. *J. Org. Chem.* **1983**, *48*, 3252–3265.

= 0.27 (20% EtOAc/ petroleum ether); $^1\text{H NMR}$ (CDCl_3) δ 7.45–7.44 (m, 2H), 7.32–7.24 (m, 3H), 5.70 (d, $J = 5.5$ Hz, 1H), 5.05 (s, 4H), 4.36–4.29 (m, 5H), 4.01–3.97 (m, 5H), 3.77–3.74 (m, 4H), 3.62 (s, 3H), 3.26 (s, 1H), 2.37 (ddd, $J = 13.1, 13.0, 5.8$ Hz, 1H), 2.18 (ddd, $J = 12.6, 12.5, 3.4$ Hz, 1H), 2.04–1.91 (m, 8H), 1.28 (d, $J = 6.4$ Hz, 3H), 1.26–1.22 (m, 12H); $^{13}\text{C NMR}$ (CDCl_3 , 125.8 MHz) δ 134.6, 131.3, 129.2, 127.2, 98.9, 98.7, 83.7, 80.4, 75.5, 67.8, 67.7, 67.6, 61.8, 60.6, 58.1, 57.0, 56.9, 55.8, 30.9, 29.8, 29.0, 21.2, 17.7, 17.5, 17.1, 14.1; HRFABMS calcd for $\text{C}_{37}\text{H}_{53}\text{O}_{10}\text{N}_{15}\text{S}$ ($\text{M} + \text{Na}^+$) 922.3718, found 922.3722.

A solution of **10** (68 mg, 0.076 mmol) in dry methylene chloride (2.7 mL) and methanol (4 mL) was cooled to 4 °C for 10 min. Mercury(II) trifluoroacetate (97 mg, 0.227 mmol) was then added and allowed to stir for 10 min. The mixture was poured into 1 N aqueous HCl (10 mL). The organic layer was washed with saturated NaHCO_3 (2×10 mL), dried over Na_2SO_4 , concentrated in vacuo, and purified by flash chromatography (20% EtOAc in petroleum ether) to afford a mixture of anomers of **11** (62 mg, 94%; 4:1 β : α). $R_f(\alpha \text{ anomer}) = 0.12$, $R_f(\beta \text{ anomer}) = 0.10$ (20% EtOAc/ petroleum ether); $^1\text{H NMR}$ (CDCl_3) δ 5.04 (d, $J = 8.2$ Hz, 4H), 4.40 (d, $J = 1.8$ Hz, 1H), 4.38–4.28 (m, 4H), 4.08–3.97 (m, 3H), 3.73 (s, 3H), 3.64–3.58 (m, 6H), 3.53–3.49 (m, 4H), 3.26 (s, 1H), 2.19 (ddd, $J = 12.4, 12.3, 9.8$ Hz, 1H), 1.31 (d, $J = 6.4$ Hz, 3H), 1.28 (d, $J = 6.4$ Hz, 3H), 1.24–1.23 (m, 9H); $^{13}\text{C NMR}$ (CDCl_3 , 125.8 MHz) δ 101.3, 99.1, 98.9, 98.7, 80.4, 75.5, 74.7, 71.6, 67.8, 61.8, 60.6, 60.0, 57.0, 56.8, 55.8, 31.5, 29.8, 29.0, 21.3, 17.7, 17.6, 17.1, 14.4; HRFABMS calcd for $\text{C}_{32}\text{H}_{51}\text{O}_{11}\text{N}_{15}$ ($\text{M} + \text{Na}^+$) 844.3790, found 844.3826.

Methyl [(((3-Amino-2,3-dideoxy-4-O-methyl- α -L-fucopyranosyl)]-(1-4)-(3-amino-2,3-dideoxy- α -L-fucopyranosyl)]-(1-4)-(3-amino-2,3-dideoxy- α -L-fucopyranosyl)]-(1-4)-(3-amino-2,3-dideoxy- α -L-fucopyranoside (12). A solution of **11** (30 mg, 0.0365 mmol) was dissolved in methanol (2 mL) and $\text{PtO}_2 \cdot 5\text{H}_2\text{O}$ (18 mg) was added. The reaction mixture was stirred vigorously under hydrogen (1 atm) and the reaction was complete after 1.5 h. The catalyst was filtered off and the filtrate was concentrated. An aqueous solution of the crude mixture was then passed over a 5 mL CM-Sephadex column equilibrated in 1 M NH_4OH and washed with water. The amine **12** was eluted with a NH_4OH gradient and washed off at 30 mM NH_4OH . Fractions containing **12** were then lyophilized overnight to provide **12** (23 mg, 90%). $R_f = 0.23$ (5:4:4:1 EtOAc/*i*PrOH/ H_2O / NH_4OH); $^1\text{H NMR}$ (CD_3OD) δ 4.94–4.87 (m, 4H), 4.42 (d, $J = 9.5$ Hz, 1H), 4.15–4.10 (m, 4H), 3.62–3.60 (m, 7H), 3.48–3.46 (m, 4H), 3.30–3.22 (m, 5H), 2.87–2.84 (m, 1H), 1.90–1.87 (m, 4H), 1.82–1.76 (m, 5H), 1.50–1.43 (m, 1H), 1.33–1.28 (m, 6H), 1.26–1.21 (m, 9H); $^{13}\text{C NMR}$ (CD_3OD , 125.8 MHz) δ 105.4, 103.3, 102.1, 102.0, 101.9, 83.6, 83.5, 83.0, 82.6, 73.4, 69.6, 69.4, 62.8, 56.8, 51.6, 47.7, 47.5, 47.4, 36.7, 35.2, 34.8, 18.0, 17.8; HRFABMS calcd for $\text{C}_{32}\text{H}_{61}\text{O}_{11}\text{N}_5$ ($\text{M} + \text{H}^+$) 692.4446, found 692.4418.

Methyl [(((3-N-((2-Aminoacetamido))-2,3-dideoxy-4-O-methyl- α -L-fucopyranosyl)]-(1-4)-(3-N-((2-aminoacetamido))-2,3-dideoxy- α -L-fucopyranosyl)]-(1-4)-(3-N-((2-aminoacetamido))-2,3-dideoxy- α -L-fucopyranosyl)]-(1-4)-(3-N-((2-aminoacetamido))-2,3-dideoxy- α -L-fucopyranoside (14). Compound **12** (23 mg, 0.033 mmol) was dissolved in DMF (1.7 mL). To this solution was first added *N,N'*-diisopropylethylamine (90 μL , 0.5 mmol) followed by 1-hydroxybenzotriazole (68 mg, 0.5 mmol), 1-(3-dimethylaminopropyl)-3-ethylcarbodiimide hydrochloride (68 mg, 0.5 mmol), and carbobenzyloxyglycine (105 mg, 0.5 mmol). The reaction was stirred for 2 h. The solvent was evaporated in vacuo, redissolved in methylene chloride, and washed with saturated NaHCO_3 (2×5 mL). The solvent was evaporated and the crude material was purified by flash chromatography (10% MeOH in CHCl_3) to give **13** (46 mg, 85%). $R_f = 0.28$ (10% MeOH/ CHCl_3); $^1\text{H NMR}$ (CDCl_3) δ 7.46–7.40 (br, 1H), 7.35–7.30 (m, 15 H), 7.17–7.15 (br, 3H), 6.30 (br, 1H), 5.80–5.72 (br, 1H), 5.52 (br, 2H), 5.16–5.06 (m, 10H), 4.89–4.83 (m, 4H), 4.46–4.39 (m, 5H), 4.21–4.11 (m, 5H), 3.88–3.82 (m, 10H), 3.59–3.54 (m, 1H), 3.48–3.42 (m, 10H), 3.22 (bs, 1H), 1.88–1.77 (m, 4H), 1.57–1.55 (m, 6H), 1.30–1.27 (m, 6H), 1.20–1.16 (m, 9H); $^{13}\text{C NMR}$ (CDCl_3 , 125.8 MHz) δ 168.8, 156.7, 136.6, 128.8, 128.7, 128.6, 128.4, 128.3, 101.6, 99.9, 79.2, 71.8, 68.3, 67.5, 67.3, 67.1, 62.3, 56.7, 48.3, 44.6, 32.9, 31.3, 30.9, 17.5;

HRFABMS calcd for $\text{C}_{82}\text{H}_{106}\text{O}_{26}\text{N}_{10}$ ($\text{M} + \text{Na}^+$) 1669.7177, found 1669.7158.

A solution of **13** was dissolved in methanol (46 mg, 0.028 mmol) and 10% Pd/C (90 mg) was added. The reaction mixture was stirred vigorously under hydrogen (1 atm) and the reaction was complete after 1.5 h. The catalyst was filtered off and the filtrate was concentrated. An aqueous solution of the crude mixture was then passed over a 5 mL CM-Sephadex column equilibrated in 1 M NH_4OH and washed with water. The amine **14** was eluted with a NH_4OH gradient and washed off at 30 mM NH_4OH . Fractions containing **14** were then lyophilized overnight to provide **14** (20 mg, 74%). $R_f = 0.27$ (5:4:4:1 EtOAc/*i*PrOH/ H_2O / NH_4OH); $^1\text{H NMR}$ (CD_3OD) δ 5.04–5.00 (m, 4H), 4.77 (br, 1H), 4.52–4.38 (m, 5H), 4.23–4.19 (m, 4H), 4.08–4.06 (m, 1H), 3.82–3.79 (m, 2H), 3.70–3.68 (m, 2H), 3.53–3.49 (m, 3H), 3.37–3.36 (m, 4H), 3.34–3.31 (m, 10H), 2.10–1.91 (m, 4H), 1.87–1.69 (m, 6H), 1.30–1.20 (m, 15H); $^{13}\text{C NMR}$ (CD_3OD , 125.8 MHz) δ 173.8, 108.1, 192.1, 99.7, 99.6, 79.9, 77.7, 77.4, 76.7, 72.5, 68.3, 61.8, 56.0, 49.2, 45.7, 45.5, 44.5, 44.2, 32.5, 30.6, 30.4, 17.7, 17.2, 17.0; HRFABMS calcd for $\text{C}_{42}\text{H}_{76}\text{O}_{16}\text{N}_{10}$ ($\text{M} + \text{Na}^+$) 999.5338, found 999.5375.

Methyl [(((3-N-((2-Guanidino)acetamido))-2,3-dideoxy-4-O-methyl- α -L-fucopyranosyl)]-(1-4)-(3-N-((2-guanidino)acetamido))-2,3-dideoxy- α -L-fucopyranosyl)]-(1-4)-(3-N-((2-guanidino)acetamido))-2,3-dideoxy- α -L-fucopyranoside (1). Compound **14** (20 mg, 0.02 mmol) was dissolved in DMF (0.5 mL). To this solution was added triethylamine (57 μL , 0.41 mmol) followed by *N,N'*-di-CBz-S-methylisothiourea (147 mg, 0.41 mmol).³³ The reaction mixture was stirred at 45 °C for 2 days. The solvent was evaporated in vacuo, redissolved in methylene chloride, and washed with saturated NaHCO_3 (2×10 mL). The solvent was evaporated and the crude material was purified by flash chromatography (10% MeOH/ CHCl_3) to give the final product with CBz protecting groups (44 mg, 85%). $R_f = 0.20$ (5% MeOH/ CHCl_3); $^1\text{H NMR}$ (CDCl_3) δ 11.62 (br, 5H), 8.91–8.87 (br, 5H), 7.54–7.52 (m, 1H), 7.35–7.26 (m, 50H), 7.20–7.18 (m, 3H), 6.21–6.20 (m, 1H), 5.18–5.16 (m, 10H), 5.10–5.04 (m, 10H), 4.88–4.81 (m, 4H), 4.51–4.50 (m, 4H), 4.39–4.37 (d, $J = 9.5$ Hz, 1H), 4.16–3.88 (m, 15H), 3.57–3.56 (m, 1H), 3.48–3.37 (m, 10H), 3.20 (br, 1H), 1.80–1.51 (m, 10H), 1.25 (d, $J = 6.1$ Hz, 3H), 1.19 (d, $J = 6.4$ Hz, 3H), 1.13 (d, $J = 6.4$ Hz, 3H), 1.10–1.08 (m, 6H); FABMS (relative intensity) *m/e* 2552 ($\text{M}^+ + \text{Na}$, 2.1), 2529 ($\text{M}^+ + 1$, 2.2).

The CBz-protected final product (44 mg, 0.017 mmol) was dissolved in MeOH (0.6 mL) and 44 mg of 10% Pd/C was added. The reaction mixture was stirred vigorously under hydrogen (1 atm) and the reaction was complete after 1.5 h. The catalyst was filtered off and the filtrate was concentrated. An aqueous solution of the crude mixture was then passed over a 5 mL CM-Sephadex column equilibrated in 1 M NH_4HCO_3 and washed with water. The pentasaccharide **1** was eluted with a NH_4HCO_3 gradient and washed off at 1 M NH_4HCO_3 . Fractions containing **1** were then lyophilized overnight to provide **1** as the HCO_3 salt (23 mg, 90%). $R_f = 0.23$ (5:4:4:3 EtOAc/*i*PrOH/ H_2O / NH_4OH); $^1\text{H NMR}$ (D_2O) δ 4.97–4.90 (m, 4H), 4.53 (d, $J = 9.5$ Hz, 1H), 4.28–4.26 (m, 4H), 4.16–4.11 (m, 4H), 3.99–3.75 (m, 14H), 3.71–3.68 (m, 2H), 3.42 (s, 3H), 3.41 (s, 3H), 3.39 (br, 1H), 1.98–1.93 (m, 3H), 1.83–1.77 (m, 6H), 1.61–1.54 (m, 1H), 1.21 (d, $J = 7.0$ Hz, 3H), 1.18 (d, $J = 10.4$ Hz, 3H), 1.16–1.10 (m, 9H); $^{13}\text{C NMR}$ (D_2O , 125.8 MHz)³⁴ δ 172.2, 172.1, 171.8, 167.1, 160.3, 103.9, 101.9, 101.7, 81.6, 80.0, 79.8, 78.8, 74.6, 70.6, 70.3, 64.4, 59.2, 53.2, 51.7, 48.4, 47.9, 46.6, 46.4, 33.6, 32.1, 26.0, 19.5, 19.1, 19.0; MS (rel intensity), *m/e* 1188 ($\text{M}^+ + 1$, 2.4), 616 ($\text{M}^+/2 + \text{Na}$, 13), 594 ($\text{M}^+/2 + 1$, 99).

Acknowledgment. This work was supported by grants GM53066 and GM42733 from the National Institutes of Health. JA992513F

(33) Tian, Z.; Edwards, P.; Roeske, R. W. *Int. J. Peptide Protein Res.* **1992**, *40*, 119–126.

(34) Indirect chemical referencing was done using chemical shift referencing ratios obtained from the following: www.bmrb.wisc.edu/ref_info/cshift.html

(35) Assignments are reported to ± 0.005 ppm accuracy. For the internal sugars B, C, and D overlap of resonances upon complexation to DNA made it difficult to measure chemical shift changes.